LETTER TO THE EDITOR

# Efficacy of the kinase inhibitor CHZ868 against *JAK2* rearrangements in pediatric acute lymphoblastic leukemia

## Authors

Manuel Quadri,[1] Claudia Saitta,[1,2] Sonia Palamini,[1,2] Stefano Rebellato,[1] Titus Watrin,[3] Jia-Wey Tu,[3] Sanil Bhatia,[3] Arndt Borkhardt,[3] Chiara Palmi,[1] Andrea Biondi,[1,4] Giovanni Cazzaniga[1,2] and Grazia Fazio[1,2]

[1]Tettamanti Center, Fondazione IRCCS San Gerardo dei Tintori, Monza, Italy; [2]School of Medicine and Surgery, University of Milano-Bicocca, Milano, Italy; [3]Department of Pediatric Oncology, Hematology and Clinical Immunology, Medical Faculty, Heinrich Heine University Düsseldorf, Düsseldorf, Germany and [4]Pediatrics, Fondazione IRCCS San Gerardo dei Tintori, Monza, Italy

Correspondence:
G. CAZZANIGA - giovanni.cazzaniga@unimib.it
G. FAZIO - grazia.fazio@unimib.it

https://doi.org/10.3324/haematol.2025.287840

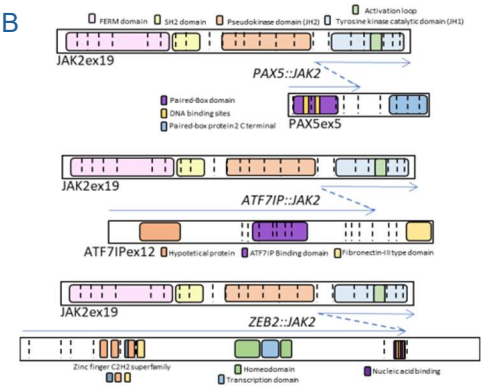
Received: May 8, 2025.
Accepted: April 9, 2026.
Early view: April 16, 2026.

©2026 Ferrata Storti Foundation
Published under a CC BY-NC license

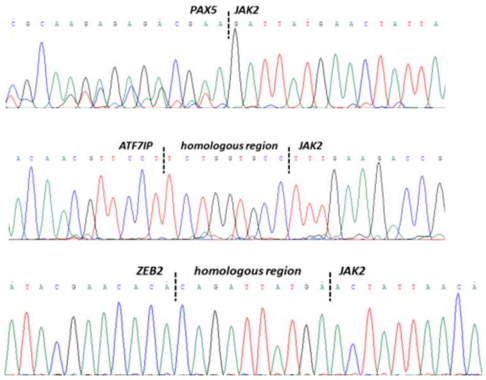
A

| Patient | Age | Phenotype | Blasts % | MRD Stratification | Protocol | JAK2R or CRLF2r | JAK2 mutational Status | Karyotype |
|---|---|---|---|---|---|---|---|---|
| Patient 1 | 2 | B-II | 80 | medium risk | 2009 | chr9::chr9PAX5::JAK2 | JAK2 wt | nk |
| Patient 2 | 6 | B-II | nk | medium risk | 2009 | chr9::chr12 ATF7IP::JAK2 | JAK2 wt | nk |
| Patient 3 | 16 | B-II | nk | medium risk | 2000-R2006 | chr2::chr9 ZEB2::JAK2 | JAK2 wt | nk |
| Patient 4 | 11 | B-II | 89 | high risk | 2017 | chr9::chr12 GIT2::JAK2 | JAK2 wt | nk |
| Patient 5 | 2 | B-II | 60 | standard risk | 2017 | chr9::chr9PAX5::JAK2 | JAK2 wt | nk |
| Patient 6 | 14 | B-II | 70 | early high risk | 2017 | chr9::chr9PAX5::JAK2 | JAK2 wt | 46,X,der(Y)(Ypter->Yq12::Y::Yq12->Yqter)[30] |
| Patient 7 | 17 | B-II | 80 | high risk | 2017 | chr9::chr9PAX5::JAK2 | JAK2 wt | nucish9p34(ABLx2),22q11.2 (BCRx2),11q23(MLLx2)(200),(ETV6x1),(RUNX1x2)(ETV6 withRUNX1 x0)(120/200) |
| Patient 8 | 4 | B-II | 82 | early high risk | 2017 | chr9::chr9PAX5::JAK2 | JAK2 wt | nk |
| Patient 9 | 12 | B-II | 95 | high risk | 2017 | chr9::chr9PAX5::JAK2 | JAK2 wt | nk |
| Patient 10 | 15 | B-II | 53 | high risk | 2009 | chr9::chr9TLE4::JAK2 | JAK2 wt | nk |
| Patient 11 | 4 | B-II | 87 | medium risk | 2017 | chr9::chr22 BCR::JAK2 | JAK2 wt | 46,XX,+X,del(9)(p13p21),idic(17)(p11),-21[8]/46,XX[2] |
| Patient 12 | 12 | B-II | 60 | standard risk | 2017 | chr9::chr17 MPRIP::JAK2 | JAK2 wt | nk |
| Positive control 1 | 4 | B-II | 85 | intermediate risk | 2009 | P2RY8::CRLF2 | JAK2 wt | nk (patient affected by Down syndrome) |
| Positive control 2 | 4 | B-II | 85 | standard risk | 2009 | P2RY8::CRLF2 | JAK2 *Lc81-Ic82 insEA* mutation | 47,XY,+21c[20] |
| Negative control 1 | 16 | B-III | 95 | intermediate risk | 2009 | absent | JAK2 wt | nk |
| Negative control 2 | 3 | B-II | 93 | standard risk | 2009 | absent | JAK2 wt | nk |

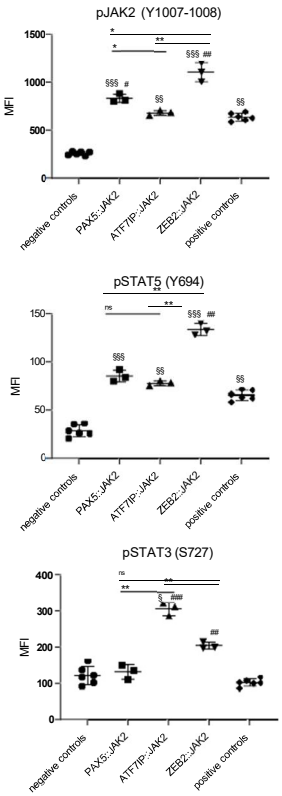
B



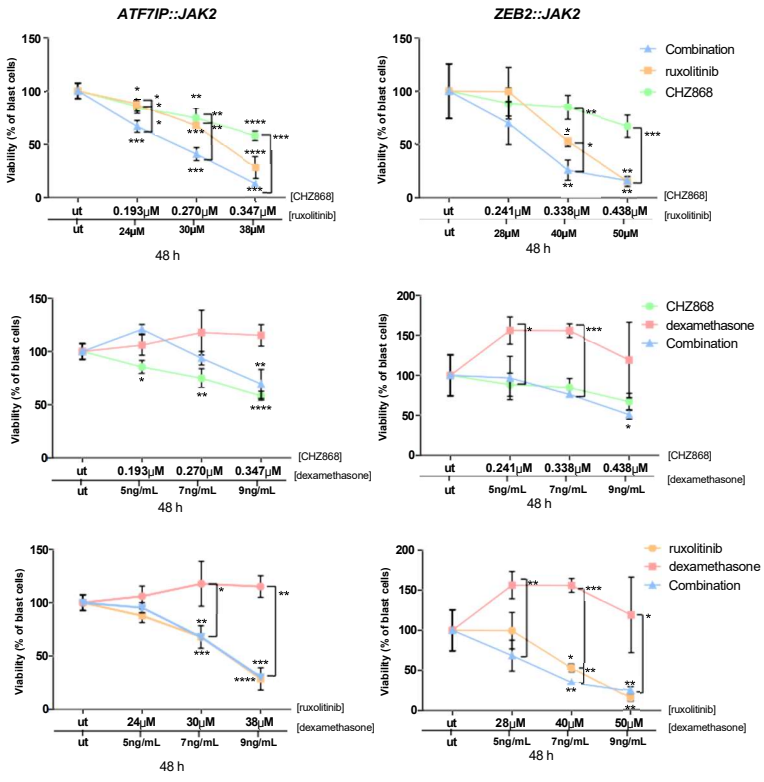

C



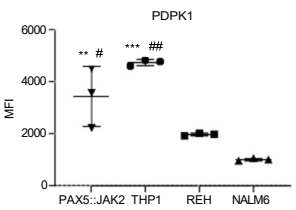

D



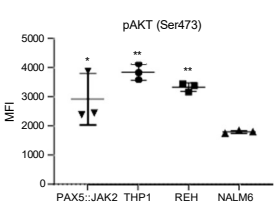

E



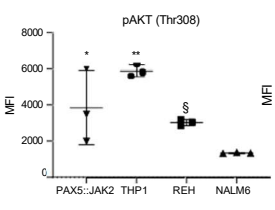

F



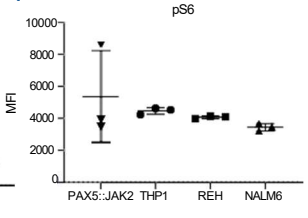

G



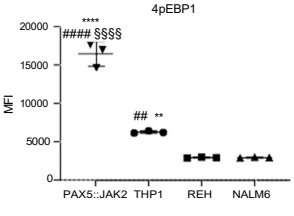

H



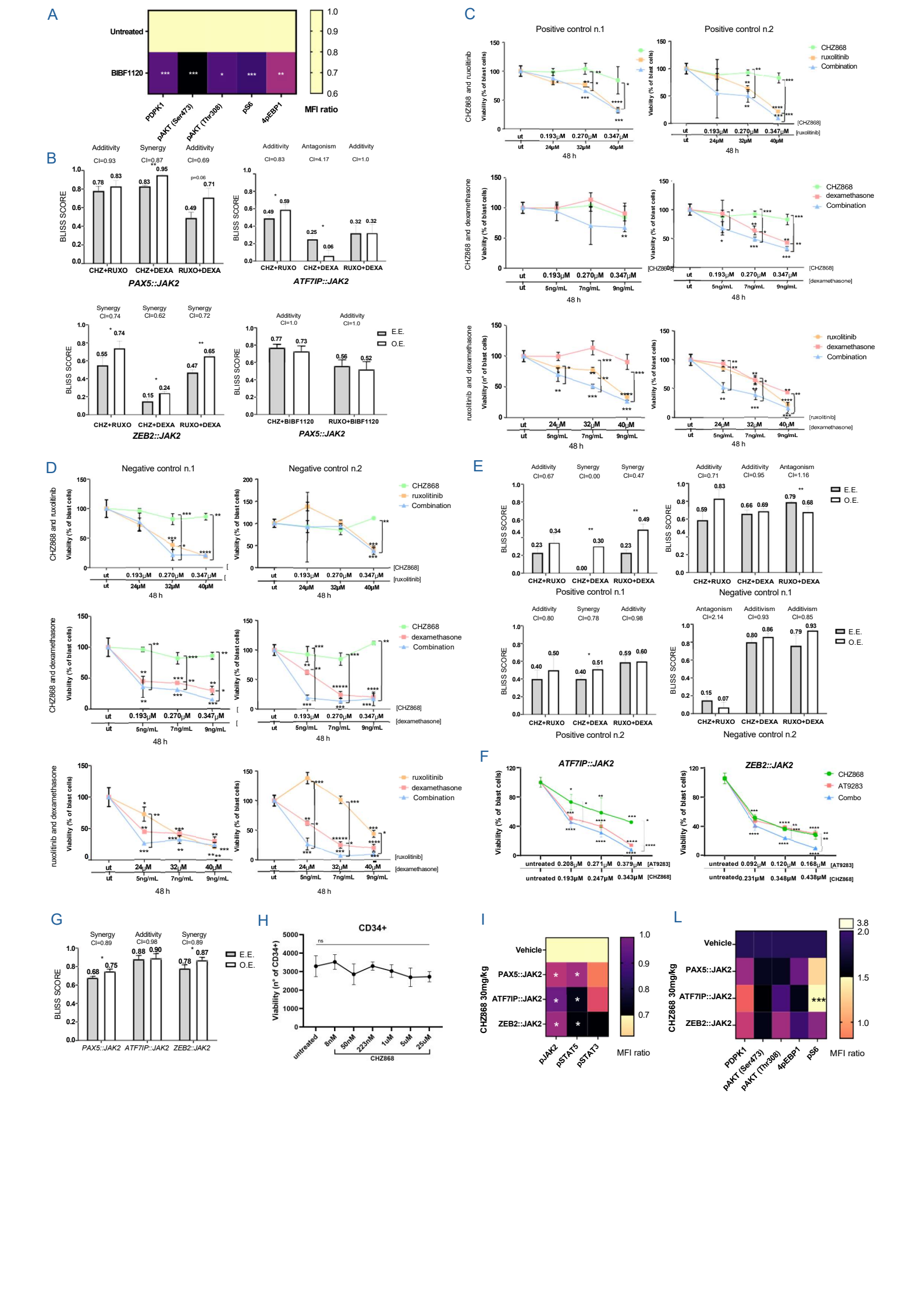

I



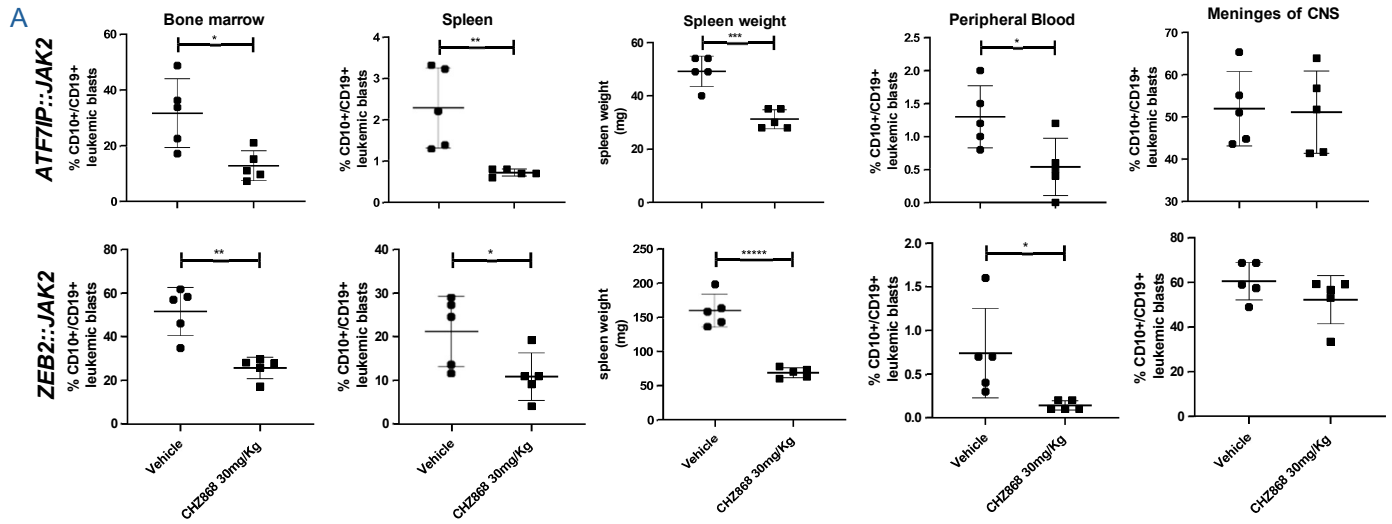

L

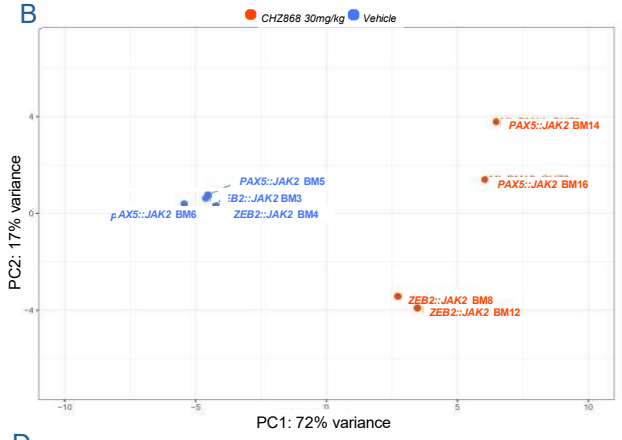


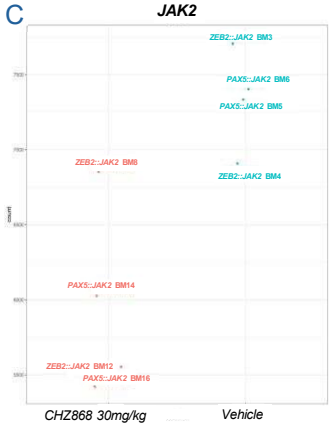
**Supplementary figure 1. Molecular and functional characterization of *JAK2* rearranged patient cohort and downstream signaling activity (A-L). A.** Cohort of JAK2r patients (patients 1-12), positive controls and negative controls identified by NGS, with summary of their main clinical characteristics, indication of the *JAK2* or *CRLF2* fusion gene, *JAK2* mutational status and karyotype. Blasts from patients 1-3 (highlighted in blue) are the ones used for the *ex-vivo* and *in-vivo* experiments. nk = not known. **B-C.** Representation of the fusion breakpoints of *PAX5::JAK2*, *ATF7IP::JAK2* and the novel *ZEB2::JAK2*, each maintaining *JAK2* tyrosine kinase catalytic domain at the end of the fusion gene, with indication of the exons and corresponding protein domains (**B**), and corresponding sanger sequences (**C**). **D**. Basal level of phosphorylation of pJAK2 (Y1007-1008), pSTAT5 (Y694), pSTAT3 (S727) of the three patients carrying JAK2r (*PAX5::JAK2, ATF7IP::JAK2, ZEB2::JAK2*) compared to n=2 positive controls, carrying one a *CRLF2* rearrangement and a $JAK2_{R683G}$ mutation, and one carrying only a *CRLF2* rearrangement, and compared to n=2 negative controls. N=3 experiments. Error bars represent standard deviation. Student's T test is shown as p values: *p<0.05; **p<0.01, ***p<0.001 among JAK2r, §p<0.05; §§p<0.01, §§§p<0.001 versus negative controls, #p<0.05; ##p<0.01, ###p<0.001 versus positive controls. **E.** *Ex-vivo* viability of $hCD10^+$ PDX-derived blasts on HBMS co-culture after 48h drugs combinations on *ATF7IP::JAK2* positive blasts (left column), indicating the decrease of viable blasts while increasing the dosages (CHZ868: 0.193µM, 0.270µM, 0.347µM; ruxolitinib: 24µM, 30µM, 38µM; dexamethasone: 5ng/mL, 7ng/mL, 9ng/mL) and on *ZEB2::JAK2* positive blasts (right column), indicating the decrease of viable blasts while increasing the dosages (CHZ868: 0.241µM, 0.338µM, 0.438µM; ruxolitinib: 28µM, 40µM, 50µM; dexamethasone: 5ng/mL, 7ng/mL, 9ng/mL). Viability was assessed from apoptosis and necrosis after staining with Annexin V-PE/7AAD and expressed as decrease of the percentage of $hCD10^+$ viable blasts (Annexin V-PE/7AAD double negative cells) and expressed as percentage of viability on untreated cells. N=3 experiments, in technical duplicate. Error bars represent standard deviation. Each column represents results on one fusion setting. The internal control is represented by untreated (ut) cells. Student's T test is shown as p values: *p<0.05; **p<0.01; ***p<0.001, ****p<0.0001. **F-L.** Basal level evaluation of the phosphorylation of PI3K-AKT pathway effectors PDPK1 (**F**), pAKT (S473) (**G**), pAKT (T308) (**H**), 4pEBP1 (**I**), pS6 (**L**), compared to THP1 and REH cell lines (high PI3K-AKT pathway expressing cells) and NALM6 cell lines (low PI3K-AKT pathway expressing cells) evaluated by phosphoflow and expressed as basal MFI. N=3 experiments. Error bars represent standard deviation. Student's T test is shown as p values: *p<0.05; **p<0.01, ***p<0.001 versus NALM6, §p<0.05; §§p<0.01, §§§p<0.001 versus THP1, #p<0.05; ##p<0.01, ###p<0.001 versus REH.

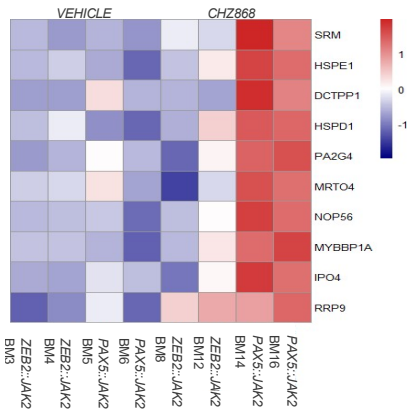

A
Untreated
BIBF1120
PDPK1
pAKT (Ser473)
pAKT (Thr308)
pS6
4pEBP1
MFI ratio
B
BLISS SCORE
CHZ+RUXO
CHZ+DEXA
RUXO+DEXA
PAX5::JAK2
ATF7IP::JAK2
ZEB2::JAK2
CHZ+BIBF1120
RUXO+BIBF1120
E.E.
O.E.
C
Positive control n.1
Positive control n.2
CHZ868 and ruxolitinib
CHZ868 and dexamethasone
ruxolitinib and dexamethasone
Viability (% of blast cells)
CHZ868
ruxolitinib
dexamethasone
Combination
48 h
D
Negative control n.1
Negative control n.2
E
Positive control n.1
Negative control n.1
Positive control n.2
Negative control n.2
F
ATF7IP::JAK2
ZEB2::JAK2
AT9283
Combo
G
H
CD34+
Viability (n° of CD34+)
CHZ868
I
Vehicle
PAX5::JAK2
ATF7IP::JAK2
ZEB2::JAK2
CHZ868 30mg/kg
pJAK2
pSTAT5
pSTAT3
MFI ratio
L
PDPK1
pAKT (Ser473)
pAKT (Thr308)
4pEBP1
pS6

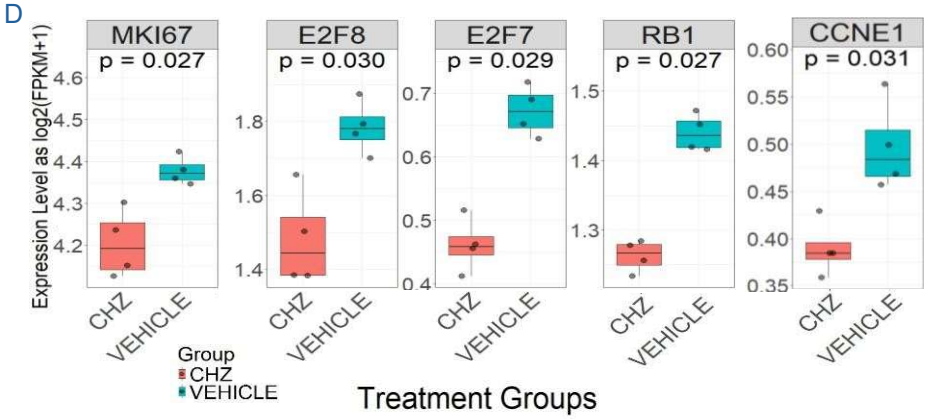
**Supplementary figure 2. Drug combination effects and signaling inhibition in *JAK2* rearranged models (A-L). A**. Heatmap expressing the mean fluorescence intensity of PI3K-AKT pathway effectors PDPK1, pAKT (S473), pAKT (T308), 4pEBP1, pS6, of 48h BIBF1120-treated *PAX5::JAK2* blasts seeded on HBMS compared to untreated blasts, evaluated by phosphoflow and expressed as MFI ratios of treated on untreated $hCD10^+$ blasts. N=3 experiments. Error bars represent standard deviation. Student's T test is shown as p values: *p<0.05; **p<0.01, ***p<0.001. **B.** 50% lethal dose **(**LD50) bliss score of the combinations of pairs of the drugs (CHZ868, CHZ; ruxolitinib, RUXO; dexamethasone, DEXA; nintedanib, BIBF1120) after 48h of treatment, indicating the ratio of apoptotic treated blasts versus untreated, which compares expected event (E.E.) and observed event (O.E.), with indication of combination index (CI) values, to evaluate synergy (p value and CI<1), additivity (no p value and CI≤0) or antagonism (CI>1). **C-D.** *Ex-vivo* apoptosis/viability assays of the combination of pairs of drugs, given at three different dosages, on primary blasts of positive controls (**C**) and negative controls (**D**), treated for 48h in co-culture on HBMS. Viability was assessed from apoptosis and necrosis after staining with Annexin V-PE/7AAD and expressed as decrease of the percentage of $hCD10^+$ viable blasts (Annexin V-PE/7AAD double negative cells) with increasing dosages of drugs. N=3 experiments, in technical duplicate. Error bars represent standard deviation. The internal control is represented by untreated (ut) cells. Student's T test is shown as p values: *p<0.05; **p<0.01; ***p<0.001, ****p<0.0001. **E**. LD50 bliss score of the combinations of pairs of the drugs (CHZ868, CHZ; ruxolitinib, RUXO; dexamethasone, DEXA), comparing expected event (EE) and observed event (OE), with indication of the combination index (CI) values, to evaluate synergy (p value and CI<1), additivity (no p value, CI≤0) or antagonism (CI>1). **F.** *Ex-vivo* viability of $hCD10^+$ PDX-derived blasts on HBMS co-culture after 48h drugs combinations of AT9283 and CHZ868, tested at three different dosages including their patient specific LD50s, on *ATF7IP::JAK2* (left graph) and *ZEB2::JAK2* (right graph) PDX-derived blasts. Viability was assessed from apoptosis and necrosis after staining with Annexin V-PE/7AAD and expressed as decrease of the percentage of $hCD10^+$ viable blasts (Annexin V-PE/7AAD double negative cells) and expressed as percentage of viability on untreated cells. N=3 experiments, in technical duplicate. Error bars represent standard deviation. The internal control is represented by untreated (ut) cells. Student's T test is shown as p values: *p<0.05; **p<0.01; ***p<0.001; ****p<0.0001. **G**. LD50 bliss score of the AT9283-CHZ868 combination, indicating the ratio of apoptotic treated blasts versus untreated, which compares expected event (E.E.) and observed event (O.E.), with indication of combination index (CI) values, to evaluate synergy (p value and CI<1), additivity (no p value, CI≤0) or antagonism (CI>1). **H.** Assessment of the safety of CHZ868 treatment at 6 dosages from 8nM to 25µM on $CD34^+$ hematopoietic stem cell (HSPCs) purified from healthy donors as determined by the absence of significant apoptosis induction by annexin V/7AAD staining. N=3 experiments, in technical duplicate. Error bars represent standard deviation. Student's T test expressed as p values: *p<0.05; **p<0.01; ***p<0.001, ****p<0.0001, *****p<0.00001. The internal control is represented by untreated cells. **I-L**. Heatmaps reporting the reduction of phosphorylation of pJAK2 (Y1007-1008), pSTAT5 (Y694) and pSTAT3 (S727) after 30mg/Kg CHZ868 *in-vivo* treatment of *PAX5::JAK2* fusion setting, of *ATF7IP::JAK2* fusion setting and of *ZEB2::JAK2* fusion setting, represented as MFI ratios on vehicle treated mice (**I**), and reporting the reduction of phosphorylation of PI3K-AKT pathway effectors [PDPK1, pAKT (S473), pAKT (T308), 4pEBP1, pS6] after 30mg/Kg CHZ868 *in-vivo* treatment of *PAX5::JAK2* setting, of *ATF7IP::JAK2* fusion setting and of *ZEB2::JAK2* fusion setting represented as MFI ratios on vehicle treated mice (**L**). At least N=5 mice per group. Student's T test expressed as p values: *p<0.05; **p<0.01; ***p<0.001. The internal control is represented by vehicle-treated mice. Statistics reported in white refers to a significant reduction of phosphorylation in CHZ868-treated mice compared to vehicle-treated mice, while statistics reported in black refers to a significant increase of phosphorylation in CHZ868-treated mice compared to vehicle-treated mice.

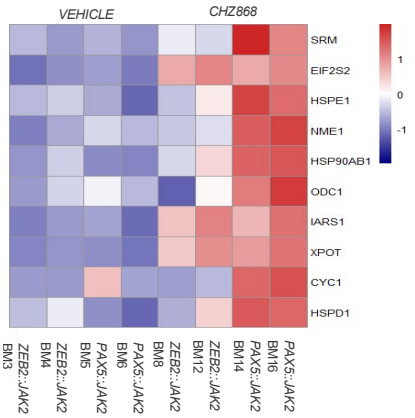

A
Bone marrow
Spleen
Spleen weight
Peripheral Blood
Meninges of CNS
ATF7IP::JAK2
ZEB2::JAK2
% CD10+/CD19+ leukemic blasts
spleen weight (mg)
Vehicle
CHZ868 30mg/Kg

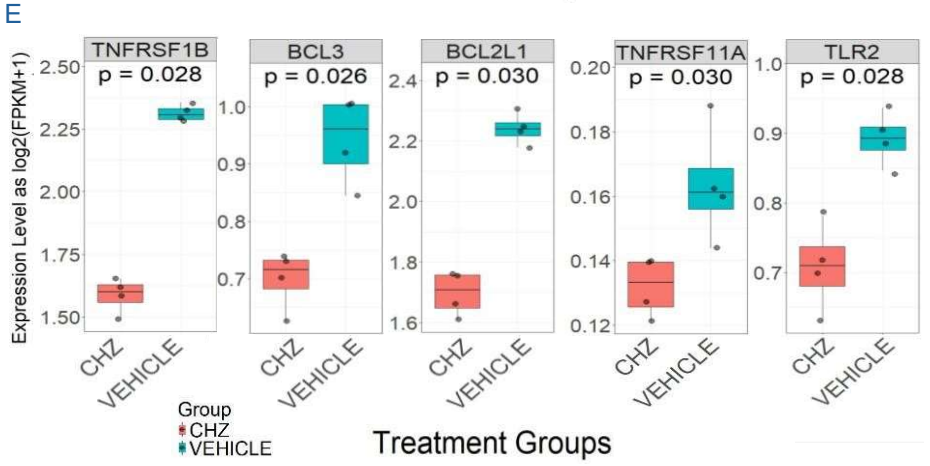

B
CHZ868 30mg/kg
Vehicle
PAX5::JAK2 BM14
PAX5::JAK2 BM16
PAX5::JAK2 BM5
ZEB2::JAK2 BM3
PAX5::JAK2 BM6
ZEB2::JAK2 BM4
ZEB2::JAK2 BM8
ZEB2::JAK2 BM12
PC2: 17% variance
PC1: 72% variance

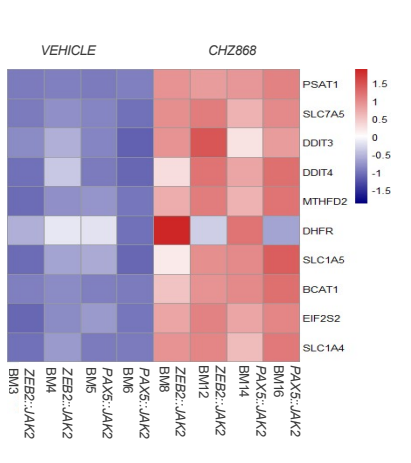

C
JAK2
CHZ868 30mg/kg
Vehicle


F
VEHICLE
CHZ868
SRM
HSPE1
DCTPP1
HSPD1
PA2G4
MRTO4
NOP56
MYBBP1A
IPO4
RRP9


D
MKI67
p = 0.027
E2F8
p = 0.030
E2F7
p = 0.029
RB1
p = 0.027
CCNE1
p = 0.031
Expression Level as log2(FPKM+1)
CHZ
VEHICLE
Group
CHZ
VEHICLE
Treatment Groups


VEHICLE
CHZ868
SRM
EIF2S2
HSPE1
NME1
HSP90AB1
ODC1
IARS1
XPOT
CYC1
HSPD1


E
TNFRSF1B
p = 0.028
BCL3
p = 0.026
BCL2L1
p = 0.030
TNFRSF11A
p = 0.030
TLR2
p = 0.028
Expression Level as log2(FPKM+1)
CHZ
VEHICLE
Group
CHZ
VEHICLE
Treatment Groups


VEHICLE
CHZ868
PSAT1
SLC7A5
DDIT3
DDIT4
MTHFD2
DHFR
SLC1A5
BCAT1
EIF2S2
SLC1A4

**Supplementary figure 3. CHZ868 *in-vivo* efficacy and consequent transcriptional profiling and pathway modulation in CHZ868-treated mice (A-F). A.** Evaluation of the reduction of the percentage of $hCD10^{+}CD19^{+}$ leukemic blasts in CHZ868-treated NSG mice compared to vehicle-treated mice, in bone marrow, spleen, peripheral blood and meninges of central nervous system (CNS), and reduction of spleen weight, in the setting of *ATF7IP::JAK2* fusion (upper row) and of *ZEB2::JAK2* fusion (lower row). At least N=5 mice for each group, treated for 10 days with washout on the weekend. Error bars represent standard deviation. Student's T test is shown as p values: *p<0.05; **p<0.01; ***p<0.001, ****p<0.0001, *****p<0.00001. **B**. Principal Component Analysis (PCA) based on gene expression profiles on n=8 samples, including n=4 vehicle-treated (blue dots) and n=4 CHZ868-treated (red dots) extracted RNA from blasts of *in-vivo* treated mice. Separation along the principal components reflects transcriptional differences induced by the treatment. **C.** *JAK2* downregulation in *in-vivo* CHZ868-treated mice (left column, red dots) compared to the higher *JAK2* expression in vehicle-treated mice (right column, blue dots) obtained by whole transcriptome analysis. **D**. Differential gene expression analysis between CHZ868-treated mice (box plots in red, 4 samples each) and vehicle-treated mice (box plots in blue, 4 samples each) on genes associated with proliferation. Five of the top significantly upregulated and downregulated genes (adjusted p-value< 0.05), with expression levels represented as $\log_2(FPKM+1)$, are reported in the figure. p-values derived from permutation-based Wilcoxon tests (10,000 permutations). **E**. Differential gene expression analysis between CHZ868-treated mice (box plots in red, 4 samples each) and vehicle-treated mice (box plots in blue, 4 samples each) on genes associated with NF-kB pathway. Five of the top significantly upregulated and downregulated genes (adjusted p-value < 0.05), with expression levels represented as $\log_2(FPKM+1)$, are reported in the figure. p-values derived from permutation-based Wilcoxon tests (10,000 permutations). **F**. Scaled expression of the top 10 genes in each hallmark [MYC V1 (upper heatmap), MYC V2 (central column), MTORC1 (right column)], sorted between-groups variance, which resulted to be correlated to a metabolic rewiring inside blasts from CHZ868-treated mice compared to blasts from vehicle-treated mice.